Proceedings of the 10th Brazilian Congress of Thermal Sciences and Engineering -- ENCIT 2004
Braz. Soc. of Mechanical Sciences and Engineering -- ABCM, Rio de Janeiro, Brazil, Nov. 29 -- Dec. 03, 2004

Paper CIT04-0791

ON THE ESTIMATION OF THE GAS-SIDE MASS-TRANSFER COEFFICIENT DURING THE FORMATION AND ASCENSION OF BUBBLES

Ricardo Carvalho Rodrigues

Cláudio Patrício Ribeiro Jr.

Paulo Laranjeira da Cunha Lage
Programa de Engenharia Química-COPPE, Universidade Federal do Rio de Janeiro P.O. Box 68502, 21945-970 Rio de Janeiro, RJ, Brasil. Fax: 55-21-25628300, paulo@peq.coppe.ufrj.br

Abstract: Using a recently developed diffusive model for the simultaneous heat and multicomponent mass transfer during the formation and ascension of superheated bubbles, concentration profiles within a bubble during the stripping of diluted ethyl acetate solutions were determined and then used in the computation of the corresponding mass-transfer coefficient on the gas side, k_G. Both isothermal and non-isothermal bubbling cases were analysed. For the studied system, the importance of the gas-side resistance to mass transfer, usually neglected in the literature, was clearly shown. During the formation stage, a large drop in k_G with time was observed, as the mean gas velocity inside the bubble decreased on account of bubble growth. On the other hand, after bubble detachment, the value of k_G remained approximately constant throughout the ascension time. In both cases, for isothermal bubbling, the definition of a mean k_G value did not lead to significant errors in the prediction of transient evolution of the mean ethyl acetate concentration in the bubble. In the case of non-isothermal bubbling, an increase in the gas inlet temperature had little effect on the ethyl acetate concentration during bubble formation, but, during the ascension stage, a faster rate of concentration increase was observed.

Keywords: bubbles, mass transfer, bubble column, gas stripping

1. Introduction

The bubbling of gases or vapours through liquids for mass-transfer purposes is a common operation in many industrial processes, such as gas absorption, humidification and gas stripping. Stirred vessels, packed towers, trickle bed reactors and bubble columns are devices extensively used in these applications. Bubble columns, in particular, exhibit many advantages over the other contactors, among which one can highlight excellent mass-transfer properties, easy temperature control, capacity of operation with solids without erosion or plugging problems, decreased capital investment, lower operating and maintenance costs and greater simplicity of construction (Shah et al., 1982; Heijnen and Van't Riet, 1984; Deckwer and Schumpe, 1993).

Most industrial applications of bubble columns involve the absorption of reagents whose concentrations in the gas phase are high or species whose solubilities in the liquid phase are low. In these cases, the main resistance to mass transfer lies in the liquid phase and, accordingly, the liquid-side mass-transfer coefficient, k_L, controls the mass-transfer resistance. Consequently, a vast amount of literature has been published on the estimation of k_L during the ascension of bubbles in the last 40 years, including both empirical correlations (Calderbank and Moo-Young, 1961; Hughmark, 1967; Akita and Yoshida, 1974; Nakanoh and Yoshida, 1980; Hikita et al., 1981; Shpirt, 1981; Öztürk et al., 1987; Wilkinson et al., 1994; Behkish et al., 2002) and mathematical models (Kawase et al., 1987; Polyanin and Vyaz'min, 1995; Ponoth and McLaughlin, 2000**)**. The formation step has also been analysed, though to a lower extent (Walia and Vir, 1976; Rocha and Carvalho, 1984; Pinheiro, 2000).

Due to the aforementioned advantages, in the last two decades, additional applications using bubble columns have been investigated, including air stripping for the removal of ammonia from wastewater (Patoczka and Wilson, 1984), removal of volatile organic compounds from water (Lionel et al., 1981; Harkins et al., 1988; Velázquez and Estévez, 1992) and, more recently, for gas stripping of aromas from fruit juices (Ribeiro Jr. et al., 2004a). On account of the dilution of the target components in the gas phase, the neglect of their diffusion within the bubble as a resistance to the overall mass-transfer process may lead to errors. Indeed, the importance of the gas-side resistance in gas stripping of diluted species has been highlighted by Pinheiro and Carvalho (1994) and Smith and Valsaraj (1997) and experimentally verified by Patoczka and Wilson (1984). For low-volatility compounds, Nirmalakhandan et al. (1992) state that the gas-phase mass-transfer coefficient, k_G, becomes more important than the one related to the liquid side. Nonetheless, only a few studies on the estimation of k_G for bubbles have been conducted, the majority of which were restricted to the bubble ascension stage (Mehta and Sharma, 1966; Filla et al., 1975; Patoczka and Wilson, 1984; Cho and Wakao, 1988). To the authors' knowledge, Rocha and Carvalho (1984) and Carvalho et al. (1986) have been the only ones to report k_G values related to bubble formation.

In this work, the matter of gas-side mass-transfer resistance during the stripping of volatile aroma compounds from

diluted aqueous solutions was addressed. With the aid of the diffusive model recently developed by Ribeiro Jr. et al. (2004b) for the simultaneous heat and multicomponent mass transfer during the formation and ascension of superheated bubbles, concentration profiles of the volatile aroma compound within the bubble were determined and then used in the computation of the corresponding k_G values throughout the bubble residence time. Both isothermal and nonisothermal bubbling cases were analysed and ethyl acetate was chosen as the model aroma compound. Moreover, a time-averaged k_G value was determined for each stage and its adequacy in representing the mass-transfer fluxes was assessed.

2. Mathematical Formulation

Most mass-transfer processes involve the contact of two or more phases and the transfer of solutes across a phase boundary. In gas stripping, for example, a solute diffuses through the carrier liquid phase to a gas surface, where it dissolves and is transferred by diffusion and/or convective mixing into the gas phase. Several mathematical models have been formulated to describe the transfer across a phase boundary. A two-resistance theory, developed by Lewis and Whitman (1924), assumes that the resistances to mass transfer are confined to two thin stagnant films on either side of the gas-liquid interface. The interface itself does not offer any resistance to solute transfer and the interfacial concentrations are, therefore, in local equilibrium and can be calculated using thermodynamic relations. The reliability of this theory has been the subject of a great amount of study and, according to Treybal (1981), a review of the obtained results indicates that the departure from equilibrium at the interface must be a rarity.

Using the two-resistance theory, the mass-transfer flux N (kg m^{-2} s^{-1}) across the interface under steady-state conditions is given by the following equation

$$N = K\left(c_L^{\infty} - \frac{c_G}{\alpha} \right) \tag{1}$$

in which α is the Henry's law constant, c_L^{∞} (kg m^{-3}) is the solute concentration in the bulk liquid phase, c_G (kg m^{-3}) is the mean concentration of solute in the gas phase and K (m s^{-1}) is the so-called overall mass-transfer coefficient, whose value is determined based on the gas- and liquid-side mass-transfer coefficients

$$\frac{1}{K} = \frac{1}{k_L} + \frac{1}{\alpha k_G} \tag{2}$$

During the stripping of a volatile compound without any chemical reaction in the gas phase, the material balance on either a forming or ascending bubble enables one to write the following relation:

$$\frac{\mathrm{d}}{\mathrm{d}t}\left(c_G V_b\right) - K A_b \left(c_L^{\infty} - \frac{c_G}{\alpha} \right) = 0 \tag{3}$$

in which V_b (m^3) and A_b (m^2) are, respectively, the bubble volume and superficial area and t (s) is time.

For an isothermal process, provided that the flux of the target component and the hydrostatic pressure head are small, bubble volume variation may be neglected in the ascension stage. In addition, if the value of K is constant, Eq. (3) can be integrated to give the variation of solute concentration in the bubble with time:

$$\frac{c_G(t) - \alpha c_L^{\infty}}{c_G^0 - \alpha c_L^{\infty}} = e^{-\xi t} \tag{4a}$$

$$\xi \equiv \frac{3K}{\alpha R_b} \tag{4b}$$

being R_b (m) the bubble radius and $c_G{}^0$ (kg m^{-3}) the mean solute concentration in the bubble for $t = 0$.

On the other hand, for the formation stage, bubble volume variation has to be taken into account. Considering isothermal bubble formation in the constant-flow-rate regime (Kumar and Kuloor, 1970), the bubble volume as a function of time is given by:

$$V_b(t) = V_0 + G_I\, t \tag{5}$$

where V_0 (m^3) is the residual bubble volume in the orifice for $t = 0$ and G_I (m^3 s^{-1}) is the gas injection flow rate. In Eq. (5), the flux of the target component is assumed to be small enough to justify the neglect of its effect upon the bubble volume.

Utilising Eq. (5), one can rewrite Eq. (3) in order to obtain the following non-linear ordinary differential equation:

$$\frac{\mathrm{d}c_G}{\mathrm{d}t} + \frac{c_G}{(V_0/G_I)+t} + \xi\left(c_G - \alpha c_L^{\infty}\right) = 0 \tag{6}$$

For a given set of K, c_L^{∞} and G_I values, Eq. (6) can be solved numerically to give the transient evolution of the mean solute concentration in the bubble during the formation stage.

2.1. Liquid-side mass-transfer coefficient

As a result of the widespread use of bubble columns in the chemical and biochemical process industries and the importance of the liquid-side mass-transfer coefficient as a design parameter for these units, a great number of empirical correlations can be found in the literature for predicting the k_L value for bubbles. After a review of the available relations, Shah et al. (1982) recommended the use of the following equation, originally proposed by Akita and Yoshida (1974) based on their data for different gas-liquid systems:

$$k_{L,i} = 0.5\frac{D_{i,L}}{2R_b}\left(\frac{\nu_L}{D_{i,L}}\right)^{\frac{1}{2}}\left(\frac{8gR_b^3}{\nu_L^{\,2}}\right)^{\frac{1}{4}}\left(\frac{4gR_b^2\rho_L}{\sigma}\right)^{\frac{3}{8}} \tag{7}$$

being g (m s^{-2}) the gravitational acceleration, $D_{i,L}$ (m^2 s^{-1}) the diffusion coefficient for species i in the liquid, ν_L (m^2 s^{-1}) the liquid kinematic viscosity, σ (N m^{-1}) the surface tension and ρ_L (kg m^{-3}) the liquid density.

In this work, in order to investigate the influence of the adopted k_L correlation upon the obtained results, apart from Eq. (7), three other relations were also tested, namely the ones proposed by Calderbank and Moo-Young (1961), Hikita et al. (1981) and Öztürk et al. (1987).

2.2. Gas-side mass-transfer coefficient

A detailed model for coupled heat and multicomponent mass transfer in bubbles, namely the one developed by Ribeiro Jr. et al. (2004b), was adopted for computing the values of k_G. According to this model, the bubble is spherical throughout its residence time in the liquid and the diffusive fluxes are appropriately described by Fick's law. In the formation stage, gas injection is modelled as a point source located at the bubble centre which emits gas at the inlet conditions. Gas property variations, as well as bubble radius changes, are taken into account. For a liquid phase containing n volatile species, this model comprises the following simplified forms of the continuity, species and energy conservation equations for the bubble:

$$\frac{\partial \rho_G}{\partial t} + \frac{1}{r^2}\frac{\partial}{\partial r}\left(r^2\rho_G v\right) = \rho_I G_I \delta(r) \tag{8}$$

$$\frac{\partial}{\partial t}\left(\rho_G Y_i\right) + \frac{1}{r^2}\frac{\partial}{\partial r}\left[r^2\rho_G\left(Y_i v - D_i\frac{\partial Y_i}{\partial r}\right)\right] = \rho_I G_I Y_{i,I}\delta(r), \qquad i = 1, 2, \ldots, n \tag{9}$$

$$\begin{aligned}&\frac{\partial}{\partial t}\left(\rho_G Cp_G T\right) + \frac{1}{r^2}\frac{\partial}{\partial r}\left(r^2\rho_G v Cp_G T\right) - \frac{1}{r^2}\frac{\partial}{\partial r}\left(r^2\lambda_G\frac{\partial T}{\partial r}\right) = \\ &\rho_I G_I \delta(r)\sum_{i=1}^{n+1} Y_{i,I}\,\overline{Cp_i^0}\,T_I + \sum_{i=1}^{n}\left(\overline{Cp_i^0} - \overline{Cp_{n+1}^0}\right)\frac{\partial}{\partial r}\left(r^2 T\rho_G D_i\frac{\partial Y_i}{\partial r}\right)\end{aligned} \tag{10}$$

in which the index $n + 1$ refers to the injected gas, assumed to be insoluble in the liquid, ρ_G (kg m^{-3}) is the gas density, r (m) is the radial coordinate, v (m s^{-1}) is the radial velocity inside the bubble, δ (m^{-3}) is the volumetric Dirac delta function, Y_i is the mass fraction of species i in the bubble, D_i (m^2 s^{-1}) is the diffusion coefficient for i in the bubble, T (K) is the temperature and λ_G (W m^{-1} K^{-1}) is the thermal conductivity of the gas mixture. The symbols Cp_G and $\overline{Cp_i^0}$ respectively refer to the heat capacities (J kg^{-1} K^{-1}) of the gas mixture and of the pure component i, whilst the index I refers to the injection condition.

Equations (8) to (10) are valid for the formation stage; the corresponding equations for the ascension stage are obtained by setting $G_I = 0$. In both cases, the relations are subjected to the following boundary conditions:

$$\frac{-\sum_{i=1}^{n}\dot{m}_i^{ev}}{4\pi R_b^2}=\rho_{G,s}\left(v_s-\frac{\mathrm{d}R_b}{\mathrm{d}t}\right)\qquad\text{at}\qquad r=R_b(t) \tag{11a}$$

$$\rho_G D_i\left.\frac{\partial Y_i}{\partial r}\right|_{r=R_b(t)}=\frac{1}{4\pi R_b^2}\left(\dot{m}_i^{ev}-Y_{i,s}\sum_{i=1}^{n}\dot{m}_i^{ev}\right)\qquad\text{at}\qquad r=R_b(t) \tag{11b}$$

$$-\lambda_G\left.\frac{\partial T}{\partial r}\right|_{r=R_b(t)}=h_L\left(T_s-T_\infty\right)+\frac{\sum_{i=1}^{n}\dot{m}_i^{ev}\left[\hat{H}_{i,G}(T_s)-\hat{H}_{i,L}(T_s)\right]}{4\pi R_b^2}\qquad\text{at}\qquad r=R_b(t) \tag{11c}$$

in which the index *s* refers to the bubble surface, T_∞ (K) is the bulk liquid temperature, h_L (W m^{-2} K^{-1}) is the convective heat-transfer coefficient outside the bubble, $\dot{m}_i^{ev}$ (kg s^{-1}) is the vaporisation rate of species *i* and $\hat{H}_i$ (J kg^{-1}) is its partial mass enthalpy in the liquid solution.

In order to predict bubble detachment from the orifice and its ascension, Eqs. (8) to (10) have to be solved together with a corresponding bubble dynamics model. As detailed by Ribeiro Jr. et al. (2004b), for the formation stage, a slight modification of the model proposed by Davidson and Schüler (1960) was utilised, whilst, for the ascension stage, a force balance was written, taking into account inertial, added mass, buoyancy and drag effects.

The simultaneous solution of Eqs. (8) to (10) gives the radial concentration profiles in the bubble for each volatile species at each time *t* up to its residence time, t_{res} (s). Therefore, the mean solute concentration in the bubble may be computed as follows:

$$c_{G,i}(t)=3\left[R_b(t)\right]^{-3}\int_0^{R_b(t)}\rho_G(r,t)Y_i(r,t)r^2\,\mathrm{d}r \tag{12}$$

Furthermore, the vaporisation rate of each component, the bubble radius, the liquid-phase concentration of component *i* at the bubble surface, $c^s_{L,i}$ (kg m^{-3}), and the Henry's law constant are also known from the solution of Eqs. (8) to (10). Thus, from the definition of the gas-side mass-transfer coefficient, it follows that:

$$k_{G,i}(t)=\frac{\dot{m}_i^{ev}(t)}{4\pi\left[R_b(t)\right]^2\left[\alpha_i(t)c^s_{L,i}(t)-c_{G,i}(t)\right]} \tag{13}$$

The $c^s_{L,i}$ value is related to $c_L{}^\infty$ by the flux relation

$$\dot{m}_i^{ev}(t)=4\pi\left[R_b(t)\right]^2 k_{L,i}\left[c^\infty_{L,i}-c^s_{L,i}(t)\right] \tag{14}$$

3. Numerical Procedure

As detailed by Ribeiro Jr. et al. (2004b), the model for coupled heat and mass transfer in bubbles was written in a dimensionless form and then solved by the method of lines using finite-volume spatial discretisation. The system of non-linear differential equations obtained after discretisation was solved together with the appropriate dynamics model utilising the DASSL routine (Petzold, 1989), whose absolute and relative tolerances were set to 10^{-10} and 10^{-8}, respectively.

In the case of isothermal bubbling, for both stages of bubble residence time in the liquid, time-averaged k_G and k_L values were computed by trapezoidal integration along the corresponding time interval. These values were substituted into Eq. (2) for calculating the respective overall mass-transfer coefficients. Once these values were known, Eqs. (4a) and (6) could be tested for the ascension and formation stages, respectively, being the latter solved by the Runge-Kutta-Verner fifth-order and sixth-order method implemented in the DIVPRK routine from the IMSL library.

All simulations were performed for the air-water-ethyl acetate system. All physical properties of the pure substances were evaluated using the correlations presented by Daubert and Danner (1985). Water-air binary diffusion coefficients as a function of temperature were calculated using the relation developed by Lage (1992), whereas the values related to ethyl acetate were estimated by the correlation of Fuller et al. (Reid et al., 1987). The ideal gas law was employed for calculating the gas mixture density, and the mixture thermal conductivity was estimated by the Mason and Saxena's modification of the Wassiljewa's equation (Reid et al., 1987). The gas mixture specific heat was computed based upon the ideal solution behaviour. For each component, the mean specific heat was obtained from its definition, using the inlet gas and liquid temperatures as the integration limits. The Henry's law constants for ethyl acetate as a function of temperature were evaluated based upon the corresponding infinite dilution activity coefficients reported by Sancho et al. (1997).

4. Results

Initially, the isothermal air stripping of a diluted ethyl acetate solution was considered. The conditions adopted to perform the simulation are detailed in Tab. 1. The simulation results for the mean concentration of ethyl acetate in the bubble and the gas-side mass-transfer coefficient are plotted in Fig. 1a as a function of the dimensionless bubble residence time, τ, defined as the ratio t/t_{res}.

Due to the mass transfer brought about by the concentration gradients between the liquid and the gas phases, the aroma concentration in the bubble increases progressively as the bubble moves through the liquid, reaching its saturation value close to the end of the ascension stage. However, a clear distinction between the rates of concentration increase related to the formation and ascension stages can be perceived, there existing a clear cusp in the concentration profile at the moment of bubble detachment. As the concentration approaches saturation, the driving force for mass transfer is reduced. Thus, the aroma mass flux to the bubble decreases and, accordingly, the rate of concentration increase falls. Even though this reasoning elucidates the individual shapes of the concentration profile in Fig. 1a for each stage of bubble residence time, it does not explain the existence of the cusp, which could be related to an augmentation of the aroma flux into the bubble after the formation stage. However, as evidenced in Fig. 1b, the aroma flux falls progressively from the formation to the ascension stages as the concentration inside the bubble increases, which is consistent with the reduction in the driving force for mass transfer. The cusp actually appears due to the interruption of gas injection into the bubble at the moment of detachment. Throughout the formation stage, aroma vaporisation into the bubble takes place in tandem with gas injection, so that the increase in the aroma amount inside the bubble is partially counterbalanced by the augmentation of the mass of inert gas, resulting in a lower net increase in the aroma concentration. At the moment of detachment, gas injection into the bubble is interrupted, and, accordingly, the previous partial counterbalance for the aroma flux into the bubble is eliminated, leading to a significant change in the concentration increasing rate, which results in the cusp in the concentration profile shown in Fig. 1a.

Table 1 - Simulation conditions adopted for the isothermal air stripping of a diluted ethyl acetate solution.

Aroma concentration in the liquid, c_L^{∞} (kg m^{-3})	1.00
Orifice diameter in the sparger, d_o (mm)	0.50
Liquid temperature, T_{∞} (K)	298.15
Gas injection flow rate in the orifice, G_I (cm^3 s^{-1})	0.3837
Pressure, P (kPa)	101.32
Bubbling height, H_b (mm)	63.3

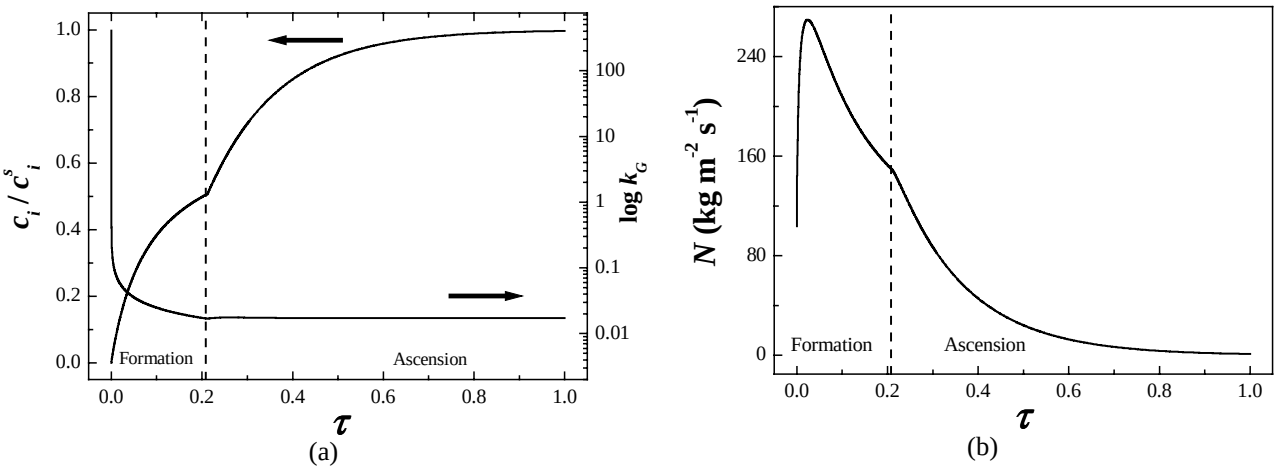

Figure 1: Simulation results for the isothermal air stripping of a diluted ethyl acetate solution: (a) mean aroma concentration in the bubble and gas-side mass-transfer coefficient; (b) aroma flux into the bubble.

With regard to the gas-side mass-transfer coefficient, the results in Fig. 1a indicate a sheer drop in this parameter at the very beginning of the formation stage. As bubble formation proceeds, this drop becomes less significant but is still considerable. In total, the k_G values for the formation stage cover almost four orders of magnitude. On the other hand, as far as the ascension stage is concerned, the changes in k_G, though still present, are much less pronounced.

The model of Ribeiro Jr. et al. (2004b), employed in this work, considers both the diffusive and the convective contributions to the radial mass flux in the bubble (see Eq. 9). The variation in k_G with the residence time is closely related to the changes in the convective contribution, which can be analysed based upon the radial velocity profiles in the bubble, whose evolution with the dimensionless residence time is portrayed in Fig. 2. At the very beginning of bubble formation, the injection flow rate is distributed within a small bubble volume, resulting in high radial velocities, which guarantee high convective fluxes, and, accordingly, high values of k_G are verified. As the bubble grows, since G_I

is kept constant throughout the formation stage, the gas radial velocity has to fall, reducing the convective contribution to the mass flux and, consequently, the value of k_G. For a constant gas injection rate, the smaller the bubble, the greater the effect of bubble growth upon the radial velocity, which accounts for the sheer drops in v, and, consequently, in k_G, observed at the very beginning of the formation stage. After the detachment, as gas injection into the bubble ceases, radial velocities can only arise from bubble volume changes brought about by either temperature variation or vaporisation fluxes. Since the analysed case is isothermal and the flux of the target component is not high enough to increase the bubble volume significantly, the radial velocity throughout the ascension stage remains approximately constant and quite close to zero, so that no significant variation in k_G is observed.

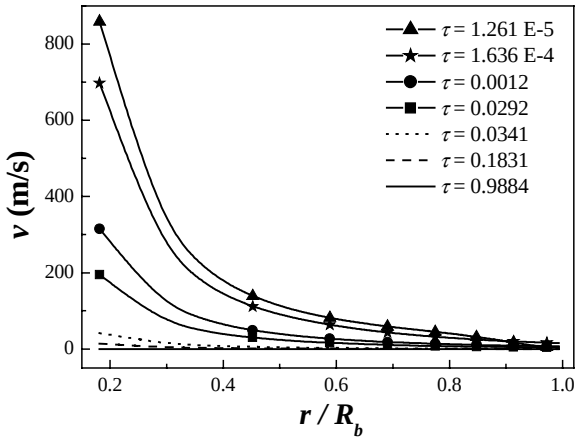

Figure 2: Radial velocity profiles for different bubble residence times during the isothermal air-stripping of a dilute ethyl acetate solution.

Another interesting aspect of Fig. 1a to which attention should be drawn is the fact that, for the studied case, even though the formation stage corresponds only to about 20% of the total bubble residence time, the aroma saturation degree reached in this stage equals 51% , clearly evidencing the importance of the formation stage to the mass-transfer process during gas sparging through liquids. This result is in perfect agreement with the observations of Carvalho et al. (1986), who have reported the formation stage to be particularly effective in those mass-transfer processes in which the gas-side resistance plays an important role.

In most practical applications, it is common to admit a constant overall resistance to mass transfer expressed in terms of a mean K value, calculated based upon mean values of k_L and k_G for the whole bubble residence time. Therefore, it is important to evaluate whether the previous results for the evolution of the mean concentration of ethyl acetate in the bubble can be reproduced using time-averaged k_G values for each bubbling stage. Following the procedure previously described in section 3, the k_G data in Fig. 1a were utilised in the calculation of the corresponding time-averaged values for both the formation and the ascension stages, which, together with time-averaged k_L values, were used for computing the mean K value in each bubbling step. Once the K values were known, Eqs. (6) and (4) were respectively used for the formation and ascension stages. The obtained profiles of the mean aroma concentration in the bubble as a function of the dimensionless residence time are compared with the ones associated with the complete model (variable K) in Fig. 3.

As evidenced in Fig. 3a, for the formation stage, despite the considerable variation in k_G with time, the assumption of a constant K whose value is calculated based upon time-averaged values does not lead to much significant errors in the prediction of the mean aroma concentration in the bubble. More specifically, at the end of the formation stage, the saturation degree calculated with the constant-K model is only 3.0% lower than the one associated with the model of Ribeiro Jr. et al. (2004b). For the ascension stage, Fig. 3b reveals that the concentration profile predicted with Eq. (4) bears considerable resemblance to the one calculated using the model of Ribeiro Jr. et al. (2004b). In this case, as the changes in the gas-side mass-transfer coefficient were much less pronounced, the time-averaged values work even better, leading to a deviation of 0.2% between the two models at the end of the ascension. Therefore, should the adequate mean values of k_G and k_L be available, mean concentration values in the bubble may be computed as a function of the residence time using Eqs. (4) and (6). Nevertheless, one should bear in mind that, in Fig. 3b, both models were solved using the same initial condition, that is, the one provided by the variable-K model for the end of the formation stage, so as to assess only the deviations intrinsic to the ascension stage. Should one solve the mass-transfer problem using the constant-K model, the errors from the formation stage will propagate to the ascension stage, increasing somewhat the discrepancies observed in Fig. 3b.

The previous outcome enables one to demonstrate the importance of the gas-side resistance to mass transfer in the considered system. For the ascension stage, keeping all other parameters constant, the overall mass-transfer coefficient K was calculated neglecting the gas-side contribution, that is, by setting $k_G = \infty$. The results thus obtained for the aroma concentration profile in the bubble are compared with the ones associated with the model of Ribeiro Jr. et al. (2004b) in

Fig. 4.

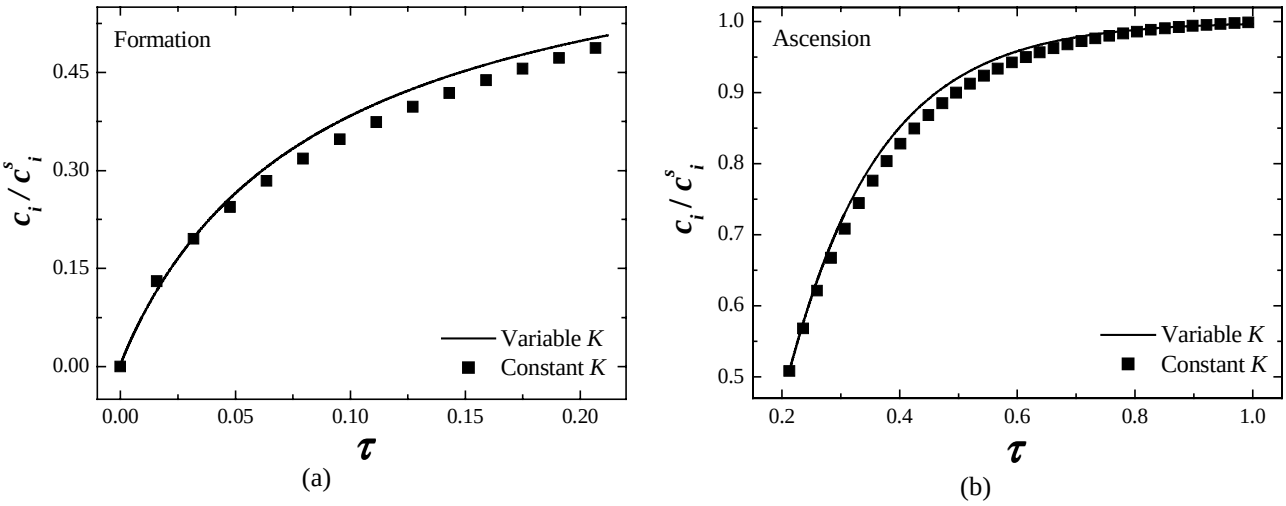

Figure 3: Comparison between the profiles of aroma concentration in the bubble predicted with the complete model (variable *K*) and the simplified one (constant *K*) for both bubbling stages: (a) formation; (b) ascension.

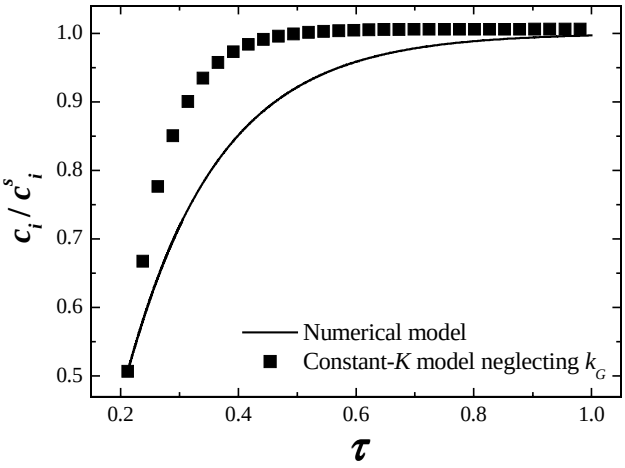

Figure 4: Analysis of the assumption of negligible gas-side mass-transfer resistance during the ascension step.

As evidenced in the aforementioned figure, for the analysed case, the neglect of the gas-side resistance during bubble ascension is rather inappropriate, leading to an overestimation of the ethyl acetate flux, and, consequently, of the aroma concentration in the bubble. When this simplification is applied, an aroma saturation degree of 98 % is obtained, for instance, before half the bubble residence time has elapsed ($\tau = 0.405$), whereas, according to the model of Ribeiro Jr. et al. (2004b), such a saturation degree can only be achieved after 71 % of the residence time.

The reason for the disagreement verified in Fig. 4 becomes clearer by means of an analysis of the individual contributions of the gas- and liquid-side resistances to the calculation of *K*, which are plotted in Fig. 5 as a function of the dimensionless residence time for both the formation and the ascension stages.

A striking aspect of the analysed process is revealed in Fig. 5, namely, an inversion of the main contributor to the overall mass-transfer resistance. At the beginning of bubble formation, on account of the high radial velocities inside the bubble and the resulting high convective fluxes, most of the mass-transfer resistance lies within the liquid phase. As the bubble grows, the radial velocities inside it decrease, causing a reduction in the k_G value, so that the gas-side contribution to the overall resistance increases. Eventually, a point is reached during the formation stage at which the individual contributions of the two phases become equal. From this point on, as the bubble keeps growing and k_G falls accordingly, the gas-side resistance surpasses the liquid-side one, corresponding to about 65% of the overall mass-transfer resistance at the moment of detachment. During the ascension stage, since bubble radius changes are small, the individual contributions from each phase remain approximately constant. Since the gas-side accounts for more than half the overall resistance to mass-transfer in the ascension stage, it is clear that its neglect will result in a considerable overestimation of the mass flux, which explains the deviations previously observed in Fig. 4. In fact, it is evident from

Fig. 5 that, but for the very beginning of the formation stage, one can not regard the mass-transfer process as one-phase controlled.

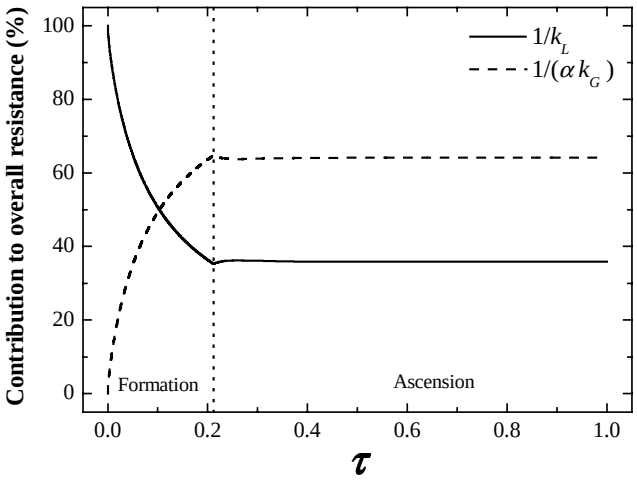

Figure 5: Individual contributions of liquid- and gas-side terms to the overall mass-transfer resistance during the isothermal air-stripping of a diluted ethyl acetate solution.

Considering the vast amount of correlations available in the literature for estimating k_L and the considerable discrepancy exhibited between some of them, an analysis of the sensitivity of the model results to the employed k_L correlation was conducted. Apart from the Akita and Yoshida (1974) correlation, utilised to obtain all results presented so far, three other correlations were tested. The simulation results for the liquid-side mass-transfer coefficient and the mean aroma concentration in the bubble are respectively portrayed in Figs. 6a and 6b.

As expected, significant differences among the k_L values estimated with different correlations are observed. All tested correlations but for the one proposed by Calderbank and Moo-Young (1961) predict an increase in k_L during the formation stage due to the augmentation of the bubble radius, whereas, for the ascension stage, an almost constant k_L value is obtained for all correlations, even though these values are only similar for the correlations of Calderbank and Moo-Young (1961) and Akita and Yoshida (1974). These differences are reflected in the mean concentration profiles, as shown in Fig. 6b. The differences are more pronounced during the formation stage, at which there is a period during which the main contribution to the overall resistance lies in the liquid phase. The higher k_L value predicted, the lower the overall resistance to mass transfer and, accordingly, the higher the aroma concentration in the bubble. In the ascension stage, as the gas-side resistance is more pronounced, the effect of k_L, though still present, becomes less important.

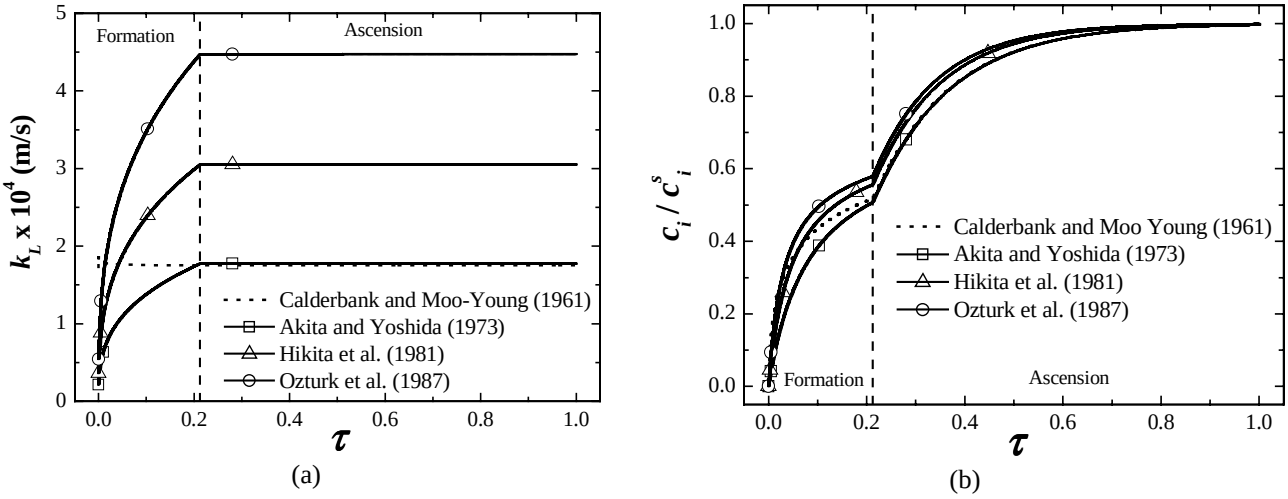

Figure 6: Simulation results for the isothermal air-stripping of a diluted ethyl acetate solution obtained with different correlations for estimating k_L: (a) liquid-side mass-transfer coefficient; (b) mean aroma concentration in the bubble.

In view of the fact that the model of Ribeiro Jr. et al. (2004b) actually considers coupled heat and multicomponent mass transfer in bubbles, non-isothermal air stripping of aromas could also be analysed. Keeping the mass flow rate of

injected gas constant, as well as the liquid temperature, simulations were performed for three different gas inlet temperatures, using the correlation of Akita and Yoshida (1974) for estimating k_L. The results for the mean aroma concentration in the bubble and the bubble mean temperature as a function of the dimensionless residence time are presented in Fig. 7. It should be emphasised that, inasmuch as the formation time is a function of the gas inlet temperature, the end of the formation stage is not indicated in Fig. 7, but it can be inferred for each case from the position of the cusp.

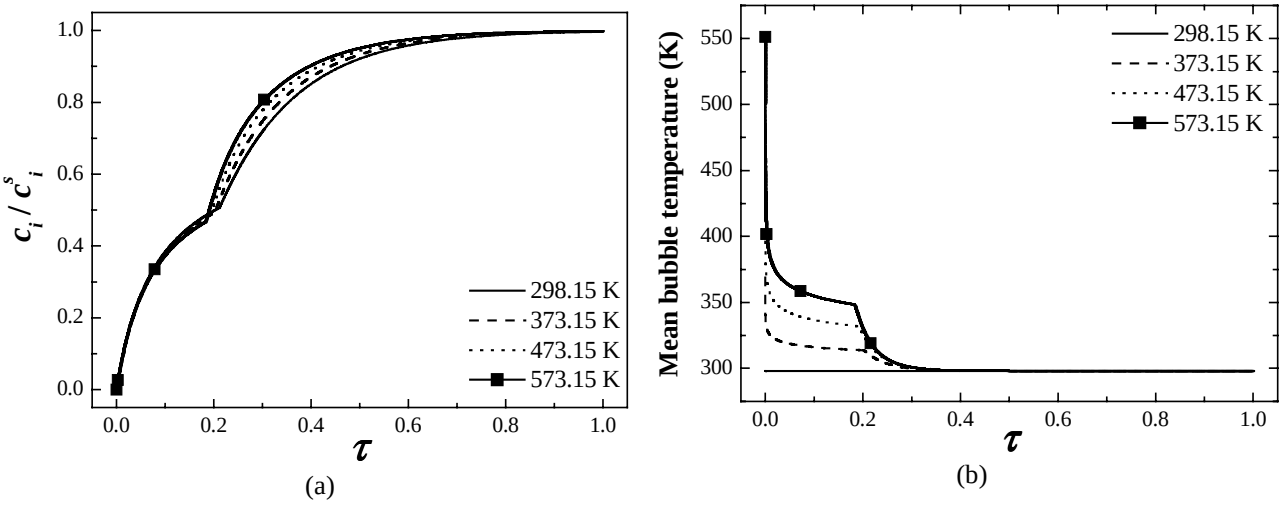

Figure 7: Simulation results for the air stripping of a diluted ethyl acetate solution using various gas inlet temperatures: (a) mean aroma concentration in the bubble; (b) mean bubble temperature.

An analysis of the results in Fig. 7a reveals that, as far as the formation stage is concerned, there is little difference between the aroma concentration obtained for the different gas inlet temperatures, even though a temperature variation of almost 300 K was considered. Nevertheless, during the ascension stage, the higher the gas inlet temperature, the faster the rate of increase of the mean aroma concentration in the bubble. As regards the bubble mean temperature, the data in Fig. 7b indicate a fast drop in the value of this parameter during the formation stage, which is a clear evidence of the high efficiency of direct-contact heat-transfer processes. In all cases, the bubble reaches the liquid temperature much before half the residence time has elapsed. Like previously observed in the mean concentration profiles, when heat transfer occurs, the mean bubble temperature profile also exhibits a cusp at the moment of detachment, whose existence is also related to the interruption of gas injection. During the formation stage, the bubble energy loss to the liquid is partially counterbalanced by the energy supplied by gas injection, which smoothes the drop in the bubble mean temperature. After detachment, since no more gas is injected into the bubble, this partial counterbalance is eliminated, and the rate of mean temperature decrease grows accordingly.

The most straightforward explanation for the changes in the concentration profiles observed in Fig. 7a would be variations in the overall mass-transfer coefficient, brought about, for instance, in view of an increase in the aroma diffusion coefficient with temperature. However, as shown in Fig. 7b, regardless of the gas inlet temperature, the mean bubble temperature is already quite close to the liquid one for values of τ as low as 0.3, while the differences in the concentration profile are still significant up to τ values of about 0.7. Actually, as evidenced by the *K* values plotted in Fig. 8a as a function of the dimensionless bubble residence time for the different gas inlet temperatures, the changes in the overall mass-transfer coefficient with the gas inlet temperature are not much significant and, more importantly, they bear little resemblance to the differences in the concentration profiles. In fact, in order to elucidate the behaviour observed in Fig. 7a, a new aspect has to be taken into account, namely, the bubble volume variations due to the gas density changes which accompany the temperature variations. This aspect is made clear in Fig. 8b, which portrays the transient evolution of the bubble radius for the four gas inlet temperatures considered in this work.

For a constant mass injection flow rate of gas, which corresponds to the case adopted in this work, an increase in the inlet temperature results in a higher volumetric injection flow rate, and, as a result, the bubble must grow faster, which is precisely the pattern verified in the first part of Fig. 8b. With a greater rate of growth, the bubble reaches the detachment condition earlier. However, due to bubble contraction caused by heat loss, the bubble volume at the end of the formation stage varies very little. These facts are all quantitatively displayed in Tab. 2. According to the data in Fig. 7b, for hot gas injection, the mean bubble temperature at the end of the formation stage is always greater than the liquid one. Therefore, as the bubble ascends, heat transfer takes place, the bubble mean temperature falls, and, on account of the resulting increase in the gas density, the bubble radius decreases, up to the point at which the liquid and the mean gas temperatures become equal. The higher the gas temperature at the detachment, the larger the extent of this effect. This reasoning is made clearer by means of a comparison between the data in Figs. 7b and 8b, which evidences that bubble radius and bubble mean temperature decreases occur within the same time interval during the ascension stage.

With the reduction in the bubble radius, the augmentation of the gas inlet temperature shortens the diffusive path, favouring mass transfer to the bubble, which is the main reason for the pattern verified in Fig. 7a during the ascension stage. The increase in the diffusion coefficient does also contribute to it, but only in the short time interval at which heat transfer takes place.

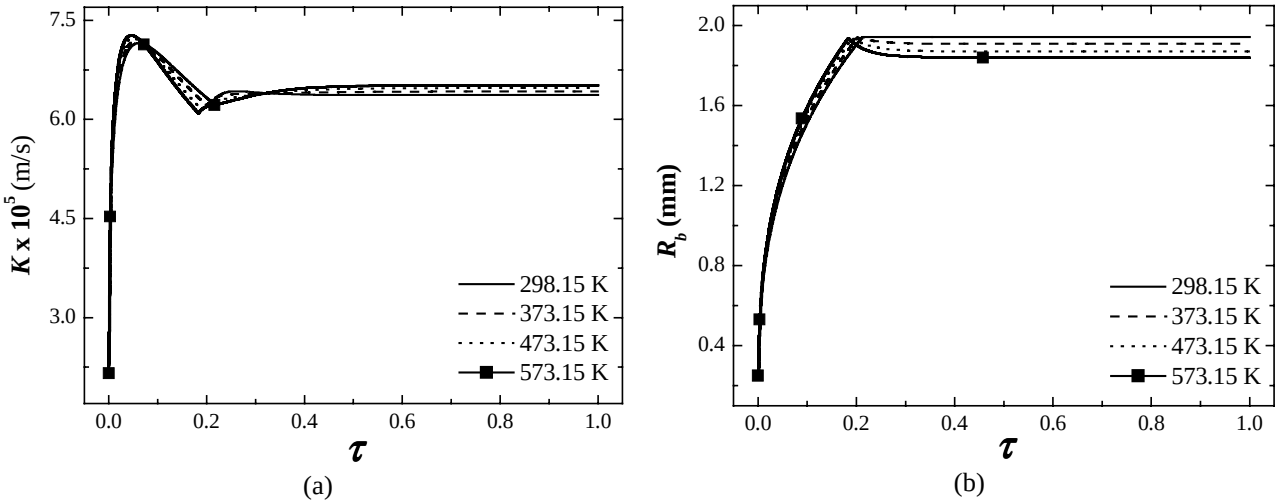

Figure 8: Transient evolution of the overall mass-transfer coefficient (a) and the bubble radius (b) during the stripping of a dilute ethyl acetate solution with different gas inlet temperatures.

Also listed in Tab. 2 are the time-averaged k_G values calculated for each gas inlet temperature considered. For the formation stage, a slight reduction in mean value of the gas-side mass-transfer coefficient is observed as the gas inlet temperature rises. Although true that, at the very beginning of the formation stage, higher volumetric flow rates ensure larger k_G values due to enhancement of the radial velocity inside the bubble, the differences between v values are fast reduced owing to the high heat-transfer efficiency. As seen in Fig 7b, almost immediately after the start of bubble growth, the maximum difference between mean bubble temperatures is already reduced to about 75 K. With regard to the ascension stage, the mean k_G value increases when the gas inlet temperature is raised, even though the effect is still small, for an almost two-fold variation in the gas temperature brings about only a 5% increment in k_G. This effect is a consequence of the reduction in the diffusive length. Indeed, the relative differences between mean bubble radius ($\overline{R_{b,res}}$) for two gas inlet temperatures are rather consistent with the ones associated with the corresponding mean gas-side mass-transfer coefficients.

Table 2 - Summary of simulation results for the air stripping of a diluted ethyl acetate solution.

T_I (K)	G_I (cm^3/s)	t_{form} (ms)	t_{res} (s)	$R_{b,\,form}$ (mm)	$\overline{R_{b,res}}$ (mm)	$\overline{k_G}$ (cm/s)	
						formation	ascension
298.15	0.3837	78.8	0.379	1.941	1.944	3.36	1.74
373.15	0.4802	74.6	0.385	1.939	1.908	3.35	1.77
473.15	0.6089	70.3	0.395	1.937	1.871	3.33	1.80
573.15	0.7376	66.9	0.406	1.936	1.840	3.32	1.83

5. Conclusions

Gas-side mass-transfer coefficients for the air-stripping of an aroma compound, namely, ethyl acetate, were calculated by means of a diffusive model for the simultaneous heat and multicomponent mass transfer during the formation and ascension of bubbles, enabling an analysis of the gas-side mass-transfer resistance in the process to be performed.

Isothermal and non-isothermal bubbling were considered in the simulations. In both cases, the formation stage was associated with a sheer drop in the k_G values, whose variation covered more than three orders of magnitude. Such variation was shown to be related to the changes in the radial velocity in the bubble and, accordingly, in the convective contribution to the mass transfer flux as the bubble grows. For the ascension stage, in contrast, an almost constant k_G was verified.

For the isothermal stripping example analysed, the individual contributions of the liquid-side and gas-side terms to the overall mass-transfer resistance were shown to vary considerably with time during the formation stage, while, for the ascension stage, they were approximately constant. Nonetheless, time-averaged k_G and k_L values were sufficient to enable reasonable predictions of the transient evolution of the mean aroma concentration in the bubble for both the

formation and ascension stages, with a relative deviation of -3.0 and 0.2% at the end of each stage, respectively. Furthermore, the importance of the gas-side resistance in the process was clearly evidenced, since the observed differences between k_L and k_G were seldom significant enough to justify the neglect of the contribution of one specific phase to the overall mass-transfer resistance.

In the case of non-isothermal stripping, an increase in the gas inlet temperature had little effect upon the transient evolution of the mean aroma concentration in the bubble during the formation stage, whilst a faster rate of aroma concentration increase was observed in the ascension stage. This effect was associated with a decrease in the diffusive path on account of the bubble contraction induced by the reduction in the mean bubble temperature as it ascended through the liquid. Time-averaged k_G values showed little dependence upon the gas inlet temperature for the formation stage in the range studied. For the ascension stage, a 5% increase in the time-averaged k_G value was observed when the gas inlet temperature was raised from 298.15 to 573.15 K.

6. Acknowledgements

The authors would like to thank CNPq (grant no. 550614/02-8) and FAPERJ (E-26/170.420/99-APQ1) for the financial support provided. Moreover, the scholarship granted to C. P. Ribeiro Jr. from FAPERJ (E-26/150.397/2004) is greatly acknowledged.

7. References

Akita, K. and Yoshida, F., 1974, "Bubble size, interfacial area and liquid-phase mass-transfer coefficients in bubble columns", Industrial and Engineering Chemistry Process Design and Development, Vol. 13, No. 1, pp. 84-91.

Behkish, A., Men, Z., Inga, J. R., Morsi, B. I., 2002, "Mass transfer characteristics in a large-scale slurry bubble column reactor with organic liquid mixtures", Chemical Engineering Science, Vol. 57, pp. 3307-3324.

Calderbank, P. H. and Moo-Young, M. B., 1961, "The continuous phase heat and mass transfer properties of dispersions, Chemical Engineering Science, Vol.16, No. 1-2, pp. 39-54.

Carvalho, J. R. F. G., Rocha, F. A. N., Vasconcelos, M. I., Silva, M. C. M. and Oliveira, F. A. R., 1986, " Mass transfer during bubbling in single and multi-orifice absorbers", Chemical Engineering Science, Vol. 41, No. 8, pp. 1987-1994.

Cho, J. S. and Wakao, N., 1988, "Determination of liquid-side and gas-side volumetric mass-transfer coefficients in a bubble column", Journal of Chemical Engineering of Japan, Vol. 21, No. 6, pp. 576-581.

Daubert, T. E. and Danner, R. P., 1985. Data compilation tables of properties of pure compounds, American Institute of Chemical Engineers.

Davidson, J. F. and Schüler, B. O. G., 1960, "Bubble formation at an orifice in a viscous liquid", Transactions of the Institution of Chemical Engineers, Vol. 38, pp. 144-154.

Deckwer, W. D. and Schumpe, A., 1993, "Improved tools for bubble column reactor design and scale-up", Chemical Engineering Science, Vol. 48 , pp. 889-911.

Filla, M., Davidson, J. F., Bates, J. F., 1975, "Gas phase controlled mass transfer from a bubble", Chemical Engineering Science, Vol. 31, pp. 359-367.

Harkins, B., Boehm, T. L. and Wilson, D. J., 1988, "Removal of refractory organics by aeration – VIII. Air stripping of benzene derivatives, Separation Science and Technology, Vol. 23, pp. 91-104.

Heijnen, J. J. and Van't Riet, K., 1984, "Mass transfer, mixing and heat-transfer phenomena in low viscosity bubble column reactors", Chemical Engineering Journal, Vol. 28, pp. B21-B42.

Hikita, H. S., Tanigawa, K., Segawa, K. and Kitao, M., 1981, "The volumetric mass-transfer coefficient in bubble columns", Chemical Engineering Journal, Vol. 22, pp. 61-67.

Hughmark, G. A., 1967, "Holdup and mass transfer in bubble columns", Industrial and Engineering Chemistry Process Design and Development, Vol. 6, No. 2, pp. 218-220.

Kawase,Y., Halard, B. and Moo-Young, 1987, "Theoretical prediction of volumetric mass-transfer coefficients in bubble columns for newtonian and non-newtonian fluids", Chemical Engineering Science, Vol. 42, No. 7, pp. 1609-1617.

Kumar, R. and Kuloor, N. R., 1970, "The formation of bubbles and drops", Advances in Chemical Engineering, Vol. 8, pp. 255-368.

Lage, P. L. C., 1992, "Vaporisation of multicomponent droplets in convective and radiant fields", D. Sc. Thesis, Rio de Janeiro, PEQ-COPPE/UFRJ, 232 p.

Lewis, W. K. and Whitman, W. G., 1924, "Principles of gas absorption", Industrial and Engineering Chemistry, Vol. 16, No. 12, pp. 1215-1220.

Lionel, T., Wilson, D. J. and Pearson, D. E., 1981, "Removal of refractory organics from water by aeration – I. Methyl chloroform", Separation Science and Technology, Vol. 16, pp. 907-935.

Mehta, V. D. and Sharma, M. M., 1966, "Effect of diffusivity on gas-side mass-transfer coefficient", Chemical Engineering Science, Vol. 21, pp. 361-365.

Nakanoh, M. and Yoshida, F., 1980, "Gas absorption by newtonian and non-newtonian liquids in a bubble column",

Industrial and Engineering Chemistry Process Design and Development, Vol. 19, No. 1, pp. 190-195.

Nirmalakhandan, N., Jang, W. and Speece, R. E., 1992, "Removal of 1,2-dibromo-3-chloropropane by countercurrent cascade air stripping", Journal of Environmental Engineering", Vol. 118, pp. 226-237.

Özturk, S. S., Schumpe, A. and Deckwer,W. D., 1987, "Organic liquids in a bubble column: hold-ups and mass-transfer coefficients",AIChE Journal, Vol. 33, No. 9, pp. 1473-1480.

Patoczka, J. and Wilson, D. J., 1984, "Kinetics of the desorption of ammonia from water by diffused aeration", Separation Science and Technology, Vol. 19, pp. 77-93.

Petzold, L. R., 1989. DASSL code, version 1989, L316, Computing and Mathematics Research Division, Lawrence Livermore National Laboratory, Livermore.

Pinheiro, M. N. C., 2000, "Liquid-phase mass-transfer coefficients for bubbles growing in a pressure field: a simplified analysis", International Communications in Heat and Mass Transfer, Vol. 27, No. 1, pp. 99-108.

Pinheiro, M.N.C. and Carvalho, J.R.F.G., 1994, "Stripping in a bubbling pool under vacuum", Chemical Engineering Science, Vol. 49, No. 16, pp. 2689-2698.

Polyanin, A. D. and Vyaz'min, A. V., 1995, "Mass and heat transfer between a drop or bubble and a flow", Theoretical Foundations of Chemical Engineering, Vol. 29, No. 3, pp. 249-260.

Ponoth, S. S., McLaughlin, J. B., 2000, "Numerical simulation of mass transfer for bubbles in water", Chemical Engineering Science, Vol. 55, pp. 1237-1255.

Reid, R. C., Praunsnitz, J. M. and Poling, B. E., 1987. "The Properties of Gases and Liquids", 4th ed., McGraw-Hill, New York, 741p.

Ribeiro Jr., C. P., Borges, C. P. and Lage, P. L. C., 2004a, "A combined gas-stripping vapour permeation process for aroma recovery", Journal of Membrane Science, Vol. 238, No. 1-2, pp 9-19.

Ribeiro Jr., C. P., Borges, C. P. and Lage, P. L. C., 2004b, "Modelling of direct-contact evaporation using a simultaneous heat and multicomponent mass transfer model for superheated bubbles", Chemical Engineering Science (accepted for publication).

Rocha, F. A. N. and Carvalho, J. R. F. G., 1984, "Absorption during gas injection through a submerged nozzle Part I: Gas-side and liquid-side transfer coefficients", Chemical Engineering Research and Design, Vol. 62, pp. 303-320.

Sancho, M. F., Rao, M. A. and Downing, D. L., 1997. "Infinite dilution activity coefficients of apple juice aroma compounds", Journal of Food Engineering, Vol. 34, pp. 145-158..

Shah, Y.T., Kelkar, B.G., Godbole, S.P., Deckwer, W.-D., 1982, "Design parameters estimations for bubble column reactors", AIChE Journal, Vol. 28, pp.353-379.

Shpirt, E., 1981, "Role of hydrodynamic factors in ammonia desorption by diffused aeration", Water Research, Vol.15, pp. 739-743.

Smith, J. S. and Valsaraj, K. T., 1997, "Bubble column reactors for wastewater treatment. 3. Pilot-scale solvent sublation of pyrene and pentachlorophenol from simulated wastewater", Industrial and Engineering Chemistry Research, Vol. 36, pp. 903-914.

Treybal, R. E., 1981, "Mass-transfer Operations", 3rd ed, Ed. McGraw-Hill, Singapore, 784p.

Velázquez, C. and Estévez, L. A., 1992, "Stripping of trihalomethanes from drinking water in a bubble-column aerator", AIChE Journal, Vol. 38, pp. 211-218.

Walia, D. S. and Vir, D.,1976, "Interphase mass transfer during drop or bubble formation", Chemical Engineering Science, Vol. 31, pp. 525-533.

Wilkinson, P. M., Haringa, H. and Dierendonck, L. L. V., 1994, "Mass transfer and bubble size in a bubble column under pressure", Chemical Engineering Science, Vol. 49, pp. 1417-1427.